

Advanced Manufacturing: Polymer & Composites Science



ISSN: (Print) (Online) Journal homepage: https://www.tandfonline.com/loi/yadm20

Process robustness and defect formation mechanisms in unidirectional semipreg

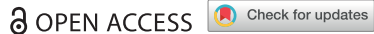
William T. Edwards, Patricio Martinez & Steven R. Nutt

To cite this article: William T. Edwards , Patricio Martinez & Steven R. Nutt (2020) Process robustness and defect formation mechanisms in unidirectional semipreg, Advanced Manufacturing: Polymer & Composites Science, 6:4, 198-211, DOI: <u>10.1080/20550340.2020.1834789</u>

To link to this article: https://doi.org/10.1080/20550340.2020.1834789

9	© 2020 The Author(s). Published by Informa UK Limited, trading as Taylor & Francis Group.
#	Published online: 16 Oct 2020.
	Submit your article to this journal $oldsymbol{oldsymbol{\mathcal{G}}}$
ılıl	Article views: 498
Q	View related articles ☑
CrossMark	View Crossmark data ☑
4	Citing articles: 1 View citing articles 🗹







Process robustness and defect formation mechanisms in unidirectional semipreg

William T. Edwards (D), Patricio Martinez and Steven R. Nutt (D)

M.C. Gill Composites Center, Viterbi School of Engineering, University of Southern California, Los Angeles, CA, USA

ABSTRACT

Out-of-autoclave/vacuum-bag-only (OoA/VBO) composite processing has emerged as an alternative to autoclave cure, addressing economic, environmental, and production flexibility limitations associated with autoclave production. VBO processing can produce defect-free components under ideal processing conditions; however, adverse process conditions (e.g. poor vacuum) commonly encountered in manufacturing environments result in unacceptably high scrap rates, preventing more widespread adoption of such techniques. This work explores how modifications to prepreg format can increase process robustness. A unidirectional (UD) prepreg was produced with a customized, discontinuous resin distribution, henceforth referred to as semipreg. The semipreg exhibited through-thickness permeability orders of magnitude greater than conventional hot-melt VBO prepregs. The semipreg also was less sensitive to variations in process conditions than conventional VBO prepreg. In situ process monitoring allowed observation and identification of two defect formation mechanisms arising during cure of the custom prepreg. Resin feature topography played a critical role in these mechanisms, indicating its importance to the design of next generation VBO semipregs.

Semipreg 5 mm 1 mm

KEYWORDS

Prepreg; semipreg; throughthickness permeability; robust manufacturing; prepreg format design; defect formation mechanism

1. Introduction

To address the growing need for rapid, flexible, robust, and cost-effective production routes for high-performance composite structures, this work aims to demonstrate that UD prepreg formats with

through-thickness gas permeability (semipregs) are less sensitive to challenging VBO processing conditions and part features (such as poor vacuum, ply drops, etc.) than commercial hot-melt prepreg. Additional objectives of this work are to identify primary mechanisms leading to defect formation during cure of semipregs and to elucidate the relationship between prepreg format and these mechanisms. The objectives are motivated by a need to inform the design of next-generation optimized semipreg formats. The study contributes to a broader goal of accelerating the adoption of VBO prepregs to reduce the environmental and economic costs of composites manufacturing associated with autoclave processing.

For use in risk-averse applications such as commercial aviation, carbon fiber reinforced polymers (CFRP) are normally processed by curing prepreg in an autoclave; however, autoclaves (1) are expensive to purchase, install, operate, and maintain, (2) require a large footprint, (3) limit production flexibility, and (4) may not accommodate large or irregular parts. VBO prepreg processing offers an alternative that retains the precise control of fiber volume fraction, fiber alignment, and availability of higher performance resins associated with prepreg processing, while replacing the autoclave with a standard oven [1].

Most VBO prepregs are produced via a solventless hot-melt process that yields prepreg with continuous resin film(s) partially or fully impregnated into one (or both) side(s) of the ply [2, 3]. A comparison of fully and partially saturated prepreg formats was first conducted in 1987 by Thorfinnson and Biermann, who showed that partially impregnated prepregs yielded nearly void-free laminates, whereas laminates made from fully saturated prepreg contained extensive porosity [4]. The difference in part quality was attributed to prepreg format: unimpregnated fibers create a network of pathways through which gases can be evacuated during cure. Evacuation through these channels, however, occurs in the plane of the ply (mainly in the fiber direction) and requires that the laminate perimeter remain permeable to gases (e.g. through use of edge breathing dams that ensure pathways are not sealed by consumables) [5].

Today, nearly all commercial OoA prepregs rely on engineered vacuum channels (EVaCs) to achieve low porosity. Such prepregs can achieve autoclaveequivalent consolidation and quality, yet require only simple ovens for cure [6]. However, oven-cure of OoA prepregs lacks the process robustness of autoclave cure, and ideal layup, bagging, and processing conditions are required [7, 8]. Part quality can also be compromised by improper handling and storage of prepregs (aging, exposure to moisture, etc.) [6, 9]. In fact, even under ideal conditions, OoA manufacturing of large parts and complex geometries remains challenging. For large parts, residual and evolved gasses must travel long distances, and

longer breathe-out distances generally correlate with higher void content [10]. This problem can be mitigated to a certain degree by employing longer vacuum holds prior to cure, but at the cost of additional out-time and slower production rates [11]. Fabrication of void-free components with complex geometries or internal ply drops can also be challenging, since evacuation paths can become occluded, resulting in higher defect levels, particularly at corners and ramps (ply drops) [12, 13].

Recently, the design of though-thickness evacuation paths into VBO prepreg has shown promise for overcoming limitations in process reliability apparent in conventional hot-melt prepregs. Semipregs feature discontinuous resin distributions and through-thickness permeability that exceeds that of conventional OoA prepregs by orders of magnitude [14]. Laminates produced with semipregs exhibited near-zero surface or bulk porosity, even under challenging process conditions [15]. The resin distribution in the semipreg was determined as a function of the fiber bed weave architecture and the roll-coating process by which it was produced. As such, the resin distribution could not be easily tailored, nor could the prepregging process be used to produce discontinuities in resin deposited on UD fiber beds. Inability to customize resin distribution irrespective of fiber bed architecture has heretofore limited the ability to conduct controlled studies to determine the relationship between semipreg format and process robustness. This limitation applies especially to UD prepregs, which comprise a significant fraction of prepreg used in aerostructures.

This work describes a lab-scale process for producing UD semipregs with controlled resin distribumeasurements of through-thickness permeability, and demonstrations that the high through-thickness permeability imparts robustness. A custom UD semipreg was designed, fabricated, characterized, and compared against a commercial VBO prepreg. The through-thickness permeability of semipreg was measured and compared against that of the commercial prepreg. Laminates were cured using both materials, and the influence of ideal and adverse conditions on part quality was investigated using microscopy and highresolution x-ray tomography to measure and map sample porosity. Two types of surface defects were identified, and in-situ monitoring of the tool-ply interface provided direct observations of the mechanisms by which each type of defect formed. The importance of minor changes in resin feature topography and the effect on void formation was demonstrated by curing laminates with modified resin features and comparing the quality of resulting laminates.

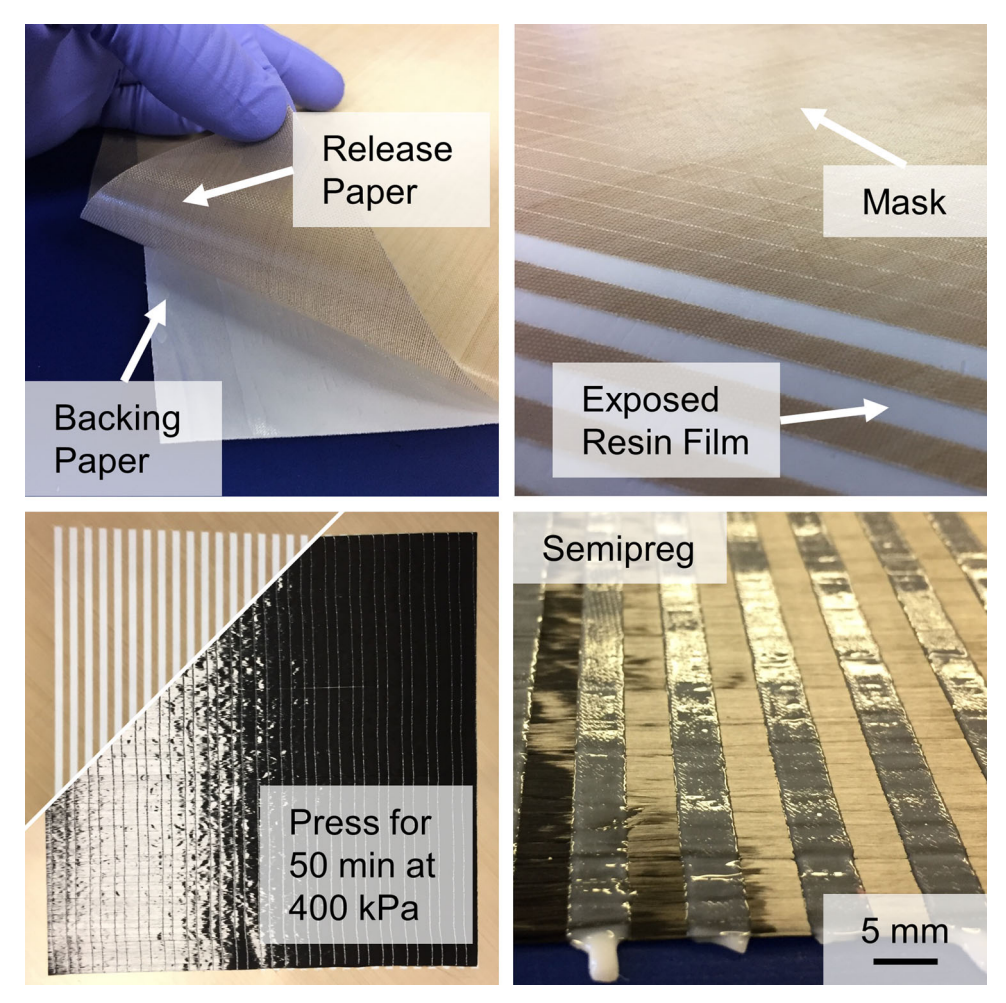


Figure 1. Key steps in the mask-and-press process used to produce semipreg.

2. Methods

2.1. Semipreg production

All through-thickness permeable prepreg was produced using a mask-and-press process to selectively transfer resin film onto a UD fiber bed. A toughened epoxy resin (PMT-F4A, Patz Materials & Technologies) was used to produce the semipreg and was procured as a continuous 152 g/m² (+/-6 g/m²) film on a backing paper. A 305-315 g/m² UD non-crimp fiber system (#2583, FibreGlast) was selected consisting of 12 K tows supported by (1) polyester threads hot-bonded (orthogonal to the fiber direction) every 8.5 mm to one side of the fabric and (2) minimal binder powder (0.7 wt. %).

Key steps of the mask-and-press prepregging process and the resulting prepreg are pictured in Figure 1. Resin film, supported by backing paper, was first covered by a release paper, then passed through an automated cutter (R19 Desktop Vinyl Cutter, Vinyl Express), which scored the release paper in a prescribed pattern. Scored regions of the release paper were removed, partly exposing the resin film beneath and creating a mask of release paper. Masked resin films were arranged on each side of a ply of UD

carbon fiber such that the release paper mask was in contact with the dry fibers. The assembly was placed in a hydraulic press (G30H-18-BCX, Wabash MPI) and pressed at 400 kPa for 50 min at room temperature (approximately 22 °C) to bond exposed resin film to each side of the fiber bed. Masks, untransferred resin film, and backing paper were then removed, resulting in a semipreg ply on which resin was distributed according to the areas removed from the scored release paper mask.

All semipreg was produced using release film masks designed such that 5.0 mm strips of resin were exposed with a periodicity of 10.0 mm, resulting in 50% coverage of the resin film by the mask. The ratio of exposed area to masked resin film area was determined in conjunction with the areal weight (or thickness) of the resin film to produce prepreg with a resin content comparable to aerospace prepreg (33 wt. %). All semipreg featured symmetric resin distribution across the midplane of each ply. Symmetry was achieved by aligning opposing masks across the fiber bed during pressing. While only one resin distribution pattern was investigated, the process described is not limited to parallel strip-type geometries and can be used to produce semipregs with various distributions (squares, dots, grids, etc.), without a requirement for periodicity. The process was tedious but was suited to lab-sale production of experimental formats, affording flexibility, affordability, and compactness, while requiring minimal resin and fabric to operate.

2.1.1. Semipreg resin topography modification

Samples of prepreg were produced via the method described in Section 2.1 and immediately modified. All modifications were intended to effect changes in the topography of semipreg resin features. To modify resin feature topography, prepreg plies were covered on both sides with a release paper and returned to the hydraulic press, where they were subjected to 400 kPa for 50 min.

Three types of release paper were used to modify the resin feature topography of semipregs: a smooth release paper, a diamond-textured release paper, and a crosshatch-textured release paper. The texture of each release paper produced changes in the morphology of resin strips on semipreg. Henceforth, unmodified prepreg produced via the mask-andpress method will be referred to as simply as semipreg while prepregs modified by subsequent pressing with smooth, diamond-textured, and crosshatchtextured release papers will be referred to as SPA, SP_B, and SP_C, respectively.

2.2. Uncured prepreg characterization

Uncured plies of semipreg were characterized to determine resin feature size and distribution, speed of through-thickness gas transport, and resin flow properties during processing. For comparison, similar characterization was conducted for a commercial UD tape prepreg (Cycom 5320-1 IM7 12 K 145gsm 33% RW UD, Cytec Solvay). The commercial prepreg characterized will be referred 'control' prepreg.

2.2.1. Resin distribution

A digital light microscope (VHX-5000, Keyence) was used to measure resin distribution on the surface of uncured plies of semipreg. Resin feature size was determined by measuring the width of each resin strip at twenty randomly selected locations (across four different plies) and averaging. To measure resin penetration into the fiber bed, samples were 'cold-cured' at room temperature in an ammonia vapor bath for 10 days [16]. After cold-curing, samples were sectioned, polished, and imaged.

2.2.2. Through-thickness permeability

Through-thickness permeability was measured for semipreg, dry UD carbon tape (#2583, FibreGlast),

and control prepreg using a custom fixture [17]. For each test, a single ply was laid over a cavity (supported by a honeycomb insert) and held in place by vacuum sealant tape. Vacuum sealant tape overlapped all sides of each ply to prevent (in-plane) gas transport through ply edges during testing. Perforated release film, breather cloth, and a vacuum bag-consumables typically used in VBO prepreg processing-were then laid up over test samples. The test fixture featured two pressure sensors (PX32B1, Omega): one connected to the cavity (on the 'cavity side' of the sample) and one connected to the volume between the vacuum bag and the sample ('bag side' of the sample).

The permeability coefficient for each sample was determined using falling pressure tests, using Darcy's Law to describe gas flow through a porous fiber bed [18, 19]. A vacuum port in the text fixture was used to apply vacuum to the bag side of the test article, while the pressure was recorded on each side of the sample. Pressure recordings were terminated when pressure on the cavity side of the sample stabilized within 1% of the pressure measured on the bag side of the sample or after 16 h.

2.2.3. Rheology

A parallel plate rheometer (AR 200ex, Instruments) was used to measure resin film viscosity. Measurements were performed over a cure cycle beginning with a 1.5° C/min ramp from room temperature to 121° C, followed by a dwell at 121° C until resin gelation occurred. This cure cycle corresponds to the cycle used to cure semipreg laminates and control material (Section 2.3). Equivalent viscosity data for the resin comprising the control material could not be measured (neat resin was not available). However, the material has been studied previously, and a model published by Kim et al. was used to estimate the viscosity profile for the control resin for comparison of resin flow properties between semipreg and control prepreg [20].

2.3. Laminate fabrication

Two studies were conducted. A Process Reliability Study was designed to determine the relationship between through-thickness gas permeability and process reliability by comparing (unmodified) semipreg against the control prepreg under challenging but commonly encountered processing conditions. A Void Formation Study was intended to determine the relationship between resin topography and void formation by comparing unmodified semipreg against semipreg that was modified as described in Section 2.1. The following subsections detail material and process conditions for the laminates produced.

2.3.1. Process reliability

Ten laminates were produced for this study: five from semipreg and five from control prepreg. Except where otherwise noted, all laminates: (1) were cured using standard consumables (edge breathing dams, perforated release film, breather cloth, vacuum bag) on a polished aluminum caul plate coated with release agent (Frekote 770-NC, Henkel); (2) measured 140 × 140 mm; (3) followed a $[0^{\circ},90^{\circ}]_{2S}$ (for semipreg) or $[0^{\circ}_{2},90^{\circ}_{2}]_{2S}$ (for control prepreg) stacking sequence; and (4) were cured using the baseline cure cycle. Laminates from the control prepreg were laid up with twice the number of plies as semipreg laminates of similar thickness $(\sim 3.2 \,\mathrm{mm})$ from the two materials. The baseline cure cycle was defined according the recommended cure cycle (for the control prepreg) and consisted of a four-hour room temperature vacuum hold (RT-VH), followed by a ramp at 1.5 °C/min to 121 °C, a two-hour dwell at 121 °C, and a ramp at -1.5 °C/ min to room temperature.

One 'Baseline' laminate was produced under baseline conditions for each prepreg. Laminates were also cured from each material under modified baseline conditions, each simulating a challenging scenario commonly encountered in industrial practice. For 'No RT Hold' laminates, baseline conditions were modified to remove the four-hour RT-VH. For 'Sealed Edges' laminates, baseline conditions were modified by replacing edge breathing dams with vacuum sealant tape placed against and over the edges of the layup. For 'Humidity Exposed' laminates, prepreg was conditioned at 90% relative humidity at 35 °C for 24 h prior to layup and cure. For 'Ply Drop' laminates, larger plies were used $(229 \times 229 \text{ mm})$ and additional plies $(90 \times 90 \text{ mm})$ were added at the midplane. Embedded plies were laid up according to $[0^{\circ},90^{\circ}]_{S}$ and $[0^{\circ}_{2},90^{\circ}_{2}]_{S}$ for semipreg and control laminates, respectively.

2.3.2. Void formation

Four laminates were produced, one from each of the four formats of unmodified and modified semipreg. Each sample was processed identically: using the baseline cure cycle, and a 100 × 100 mm, twoply, [0°, 90°] layup was cured from each of semipreg, SPA, SPB, and SPC. Laminates were cured on a glass tool plate coated with release agent using standard consumables. The interface between the tool plate and the prepreg was monitored and recorded during cure using a digital camera.

2.4. Laminate characterization

2.4.1. Thickness uniformity

The uniformity of laminate thickness was examined for several laminates produced from control prepreg and semipreg. Laminate thickness was measured every 11.3 µm along ten 35 mm long lines (five oriented along the fiber direction of the bag side ply, five oriented perpendicular to the fiber direction of the bag side ply) using a digital light microscope.

2.4.2. Bulk porosity

The bulk porosity was measured for each laminate as part of the Process Reliability Study. Two measurements were performed on polished sections $(200 \times 3.2 \text{ mm})$ from the center of each laminate and averaged to produce an indicator of laminate quality. Porosity was determined for each section by binarizing the images to distinguish pores, then dividing the pore area by the total cross section area of the laminate.

2.4.3. Micro-CT

A $24 \times 62 \times 3.2 \,\mathrm{mm}$ volume of cured semipreg was imaged with high-resolution x-ray microtomography (XT H 225ST, Nikon) using Mo-Kα incident radiation ($\lambda = 0.071$ nm, $50 \text{ kV}/400 \mu$). The scan yielded material density data at a resolution of 1.086 µm per voxel. Software (Visual Studio Max) was used to analyze microtomography data (1) to corroborate bulk defect measurements, (2) to visualize the size, shape, and distribution of voids, and (3) to identify the presence and distribution of resin-rich regions.

2.4.4. Surface quality

Surface quality was measured for all laminates. The percentage of the tool-side surface covered in defects was determined by imaging the laminate, binarizing the images to distinguish between defective and defect-free areas, and calculating the percentage of the surface with defects. A digital microscope (Edge AM7815MZTL, Dino-Lite Digital Microscope, USA) was used to capture images of the entire surface of each laminate (20x magnification) with each image corresponding to a 25.4 × 25.4 mm region. The representative surface defect content for each laminate was determined by averaging the defect levels across all images of the same laminate.

3. Results and discussion

3.1. Uncured prepreg characterization

3.1.1. Resin distribution

Measurements of resin strips on semipreg indicated that the mask-and-press process produced an average resin strip width of 5.3 mm (standard deviation

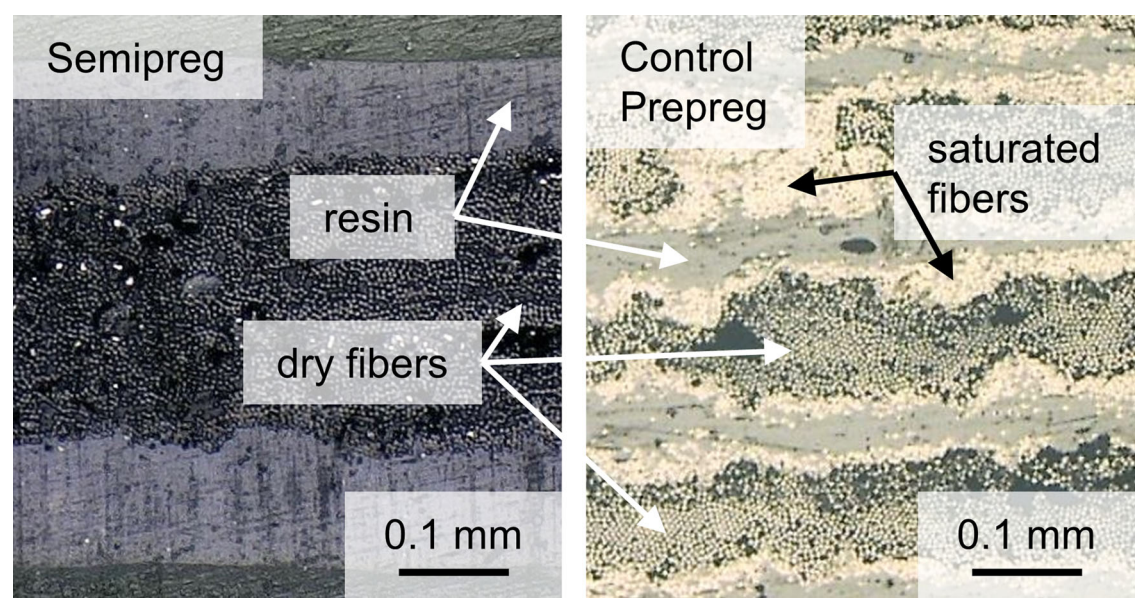


Figure 2. Micrographs of cross sections from cold-cured semipreg and control prepreg at equivalent scale.

of 1.2 mm). The 5% increase in strip width over the mask geometry was attributed to resin film stretching and tearing when excess film was removed after pressing. Each resin strip exhibited distinct edges, and strip surfaces were smooth and roughly planar. Control prepreg was characterized by continuous resin films on each ply surface. No dry fibers were exposed on control prepreg plies and resin film exhibited greater surface roughness than observed in semipregs.

As shown in Figure 2, cold-cured samples indicated no resin penetration into the fiber bed of uncured semipreg (zero initial degree of impregnation). By contrast, the uncured control material was 5-100% impregnated, depending on location.

3.1.2. Modified resin topography

Samples of semipreg pressed with textured release paper retained periodic resin distribution but changes in strip cross section or surface features were observed. Figure 3 shows surface height maps of uncured and modified semipreg samples, where bluer hues indicate lower regions of the surface (thinner regions of the ply), and yellower hues indicate higher regions (thicker). Figure 3 also shows diagrams approximating each resin strip cross section. Plies of SPA, created by pressing samples of semipreg between smooth sheets of release paper, exhibited smoother transitions in ply thickness from dry fiber to resin strip compared to the step-like change in ply thickness in semipreg. Resin strip morphology changes also resulted in average resin strip widths \sim 10% wider in SP_A than semipreg. Resin strips on SP_B, created by pressing samples of semipreg between diamond-textured release paper, exhibited periodic diamond-shaped depressions on the resin strips. Resin strips on SP_C, created by

pressing samples of semipreg between crosshatchtextured release paper, exhibited crosshatched depressions on all resin strips. These depressions, however, generally exhibited more rounded edges than on diamond-shaped features on SP_B. No change in average strip width was observed after modification of semipreg to SPB or SPC.

3.1.3. Z permeability

Gas transport in the through-thickness (z) direction was most rapid through dry fibers, reaching a pressure difference across the ply of $< 1 \, \text{kPa}$ in $\sim 30 \, \text{s}$. Gas transport was similarly rapid in the throughthickness direction of semipreg. The presence of resin strips slowed gas transport, but a pressure difference of < 1 kPa across the ply was observed after $\sim 200 \, \text{s}$. The continuous resin films covering both sides of the fiber bed in control prepreg slowed the transport of gas in the z-direction. Falling pressure tests were terminated after 16 h, at which time the pressure difference across the ply was $\sim 25\,\mathrm{kPa}$.

Test data yielded permeabilities of 4.2E-9 m², 7.1E-10 m², and 1.5E-16 m² for dry fibers, semipreg, and control prepreg, respectively. Control prepreg permeability measurements corroborate prior work characterizing the permeability of commercial VBO prepregs [15, 19, 21, 22]. Differences in throughthickness permeability between control and semipreg demonstrate the effectiveness of interrupting the continuity of resin films common to VBO prepregs for increasing the efficiency of gas transport in the through-thickness direction of a prepreg ply.

3.1.4. Rheology

Figure 4 shows resin viscosity profiles as a function of time for the relevant period of the baseline cure cycle. The control prepreg resin reached a lower

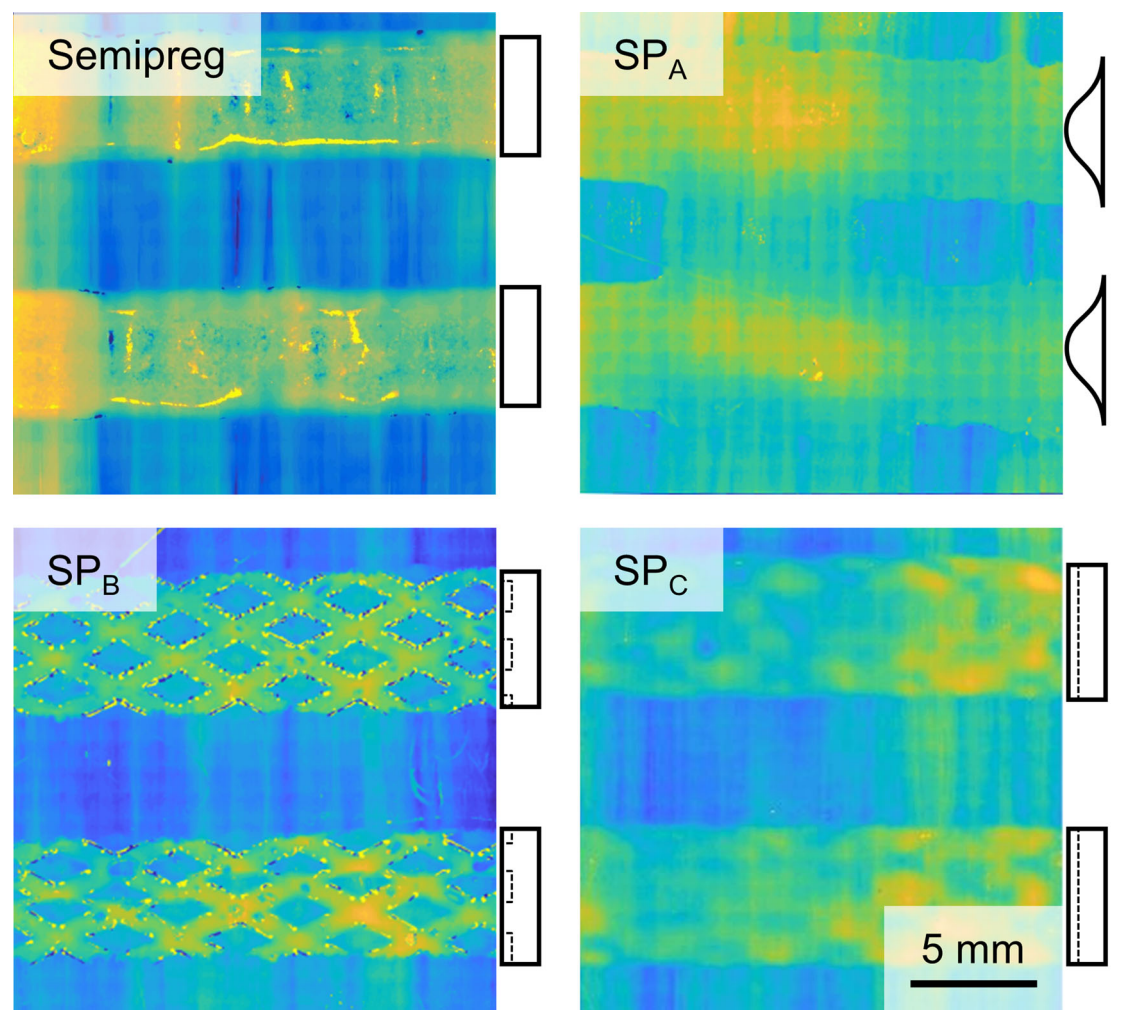


Figure 3. Morphology of modified and unmodified semipreg resin strips with diagrams showing resin strip cross section for each.

minimum viscosity (2.84 Pa s) during processing than resin comprising semipreg (5.90 Pa s) and remained at lower viscosity for a longer period than the resin comprising the semipreg.

3.2. Process reliability study

The robustness of semipreg against commonly encountered adverse processing conditions was compared against that of the control prepreg by evaluating the quality of the laminates produced from each material.

3.2.1. Bulk porosity

Average bulk porosity measurements for semipreg and control prepreg are shown in Figure 5, where error bars indicate standard deviations. Under all processing conditions, semipreg laminates exhibited bulk porosity of < 2%, a common pass/fail threshold for aerospace parts [23]. The Humidity Exposed semipreg laminate had the lowest bulk porosity at 0.30%, closely followed by the Baseline laminate at 0.46% and the Ply Drop laminate at 0.51%. Void content was greatest in No RT Hold and Sealed Edges samples.

Control prepreg cured under baseline conditions exhibited the lowest void content of any sample at 0.05%; however, the void content of laminates produced from control prepreg was more sensitive to processing conditions than laminates produced from semipreg. Bulk porosity increased to 0.81% in the No RT Hold control laminate. Void content in control prepreg laminates measured > 2% for Humidity Exposed (2.61%) and Ply Drop (3.36%) samples. Void content in control laminates was most sensitive to occlusion of the in-plane evacuation pathways: the Sealed Edge control laminate exhibited nearly 8% porosity (7.8%).

The location of bulk defects in the Baseline semipreg laminate correlated with the locations of resin strips on constituent plies. Microtomography data were used to generate a map of the projected locations of all voids in the baseline semipreg laminate (Figure 6(A)). Images in Figure 6 are oriented such that the structure is viewed in the through-thickness (z) direction. Voids in semipreg laminates were distributed along a square grid (Figure 6(A)) with a period roughly equal to the resin strip spacing.

The relationship between resin strip location/ orientation and void location was determined using

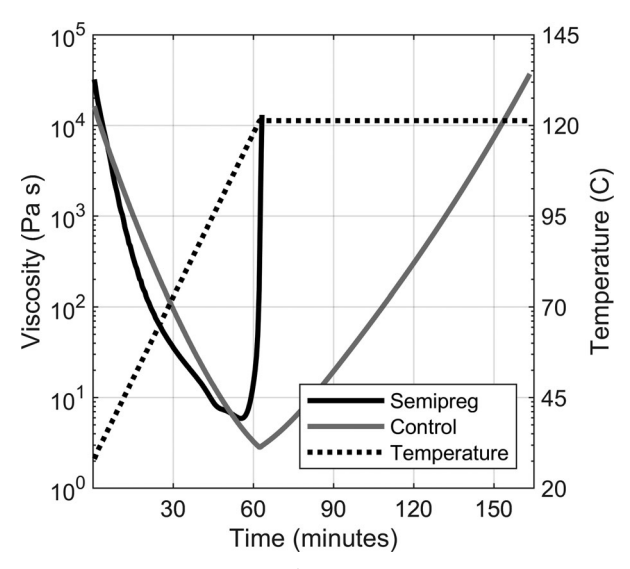


Figure 4. Resin viscosity for semipreg and control prepreg resins.

the microtomography data to isolate the 0.3 mm thick interface region between plies 2 and 3 in the layup. Figure 6(B) highlights a projection of the resin-rich regions in this volume, and a projection of the voids in the same volume is pictured in Figure 6(C). Voids are distributed along horizontal lines that correspond roughly to the location of the horizontal resin strips.

3.2.2. Surface porosity

Average surface porosity measurements for semipreg and control prepreg are shown in Figure 7, where error bars indicate standard deviations. Under all processing conditions, semipreg laminates exhibited defects on no more than 0.95% of the surface. Like bulk porosity results, the Humidity Exposed semipreg laminate exhibited fewer surface defects than any other semipreg laminate (0.20%). Large error bars on the data in Figure 7 indicate that surface quality was locally variable for all semipreg laminates, and the relative difference in quality between Baseline, No RT Hold, Sealed Edges, and Internal Ply Drop semipreg samples was negligible. The surface porosity of semipreg samples was insensitive to all processing conditions studied.

Despite producing the laminate with the fewest surface defects (0.05%), the surface quality of parts fabricated from control prepreg was strongly influenced by variations in process conditions. Surface porosity increased most modestly over Baseline conditions in the No RT Hold control laminate, which measured 0.41% surface porosity. Surface defect levels in laminates produced from control prepreg were strongly sensitive to occlusion of gas evaluation pathways (Sealed Edges), introduction of moisture (Humidity Exposed), and the addition of an internal ply drop (Ply Drop). Average surface porosity for

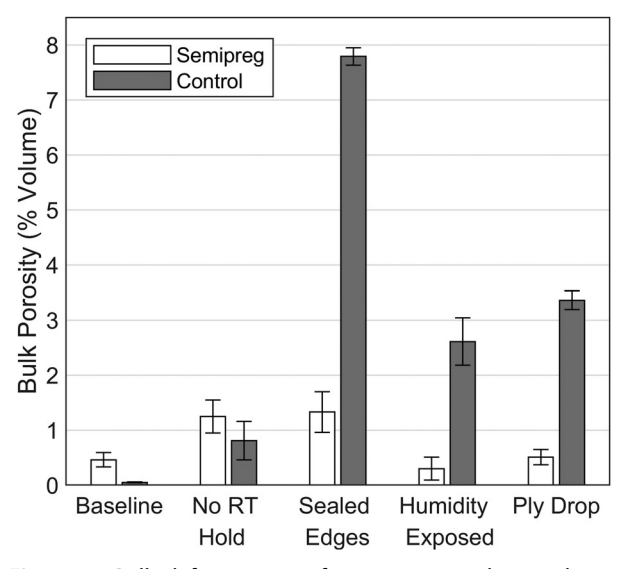


Figure 5. Bulk defect content for semipreg and control prepreg laminates produced under baseline and a variety of adverse conditions.

these processing conditions was between 9.9% and 18.5%.

Inspection of semipreg laminate surfaces revealed two distinct categories of surface defects. Figure 8 shows an image of the surface of the Ply Drop semipreg laminate with each type of defect indicated. Type 1 defects were each located near the midline of a resin strip, and their distribution was approximately periodic (10 mm period) along and across resin strips. Type 2 defects were distributed along lines between adjacent strips. Individual Type 2 defects were typically much smaller than individual Type 1 defects, but collectively accounted for 45-75% of total surface defect content. On all samples except for the Humidity Exposed laminate, Type 2 defects covered 0.3-0.5% of the laminate surface. For the Humidity Exposed laminate, however, Type 2 defect content was only one tenth that of other samples (0.08%). The difference in size, location, and distribution between Type 1 and Type 2 defects indicated that different mechanisms govern the formation of each void type. Such mechanisms are explored in Section 3.3.

3.2.3. Discussion

Bulk and surface porosity measurements demonstrate that semipreg is less sensitive to deviations from baseline process conditions than control prepreg. The quality difference between semipreg and control laminates was attributed to the presence of through-thickness gas evacuation pathways present in semipreg, which increased the speed of gas removal. Compared to control prepreg, semipreg layups had (1) more paths and (2) shorter paths $(\leq 3.2 \,\mathrm{mm} \,\mathrm{along} \,\mathrm{z\text{-}axis} \,\mathrm{vs.} \,\leq 70 \,\mathrm{mm} \,\mathrm{along} \,\mathrm{x\text{-}or} \,\mathrm{y\text{-}}$ axis) for removal of entrapped and evolved gases.

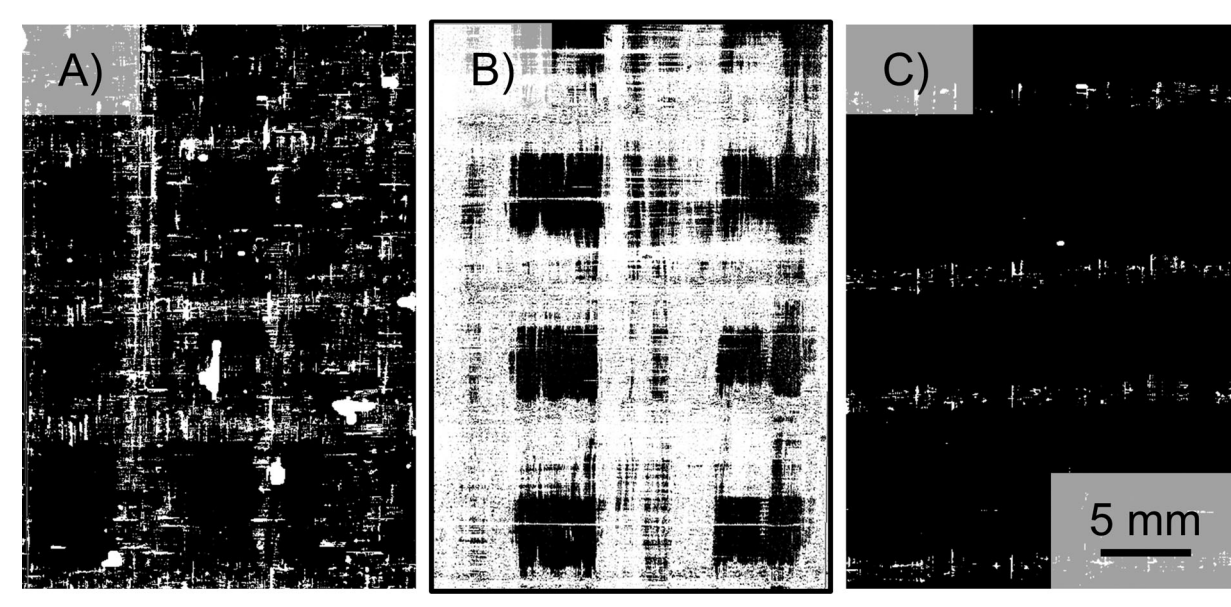


Figure 6. Microtomography data from the Baseline semipreg laminate highlighting (A) all pores, (B) resin rich volumes between plies 2 and 3, and (C) pores between plies 2 and 3.

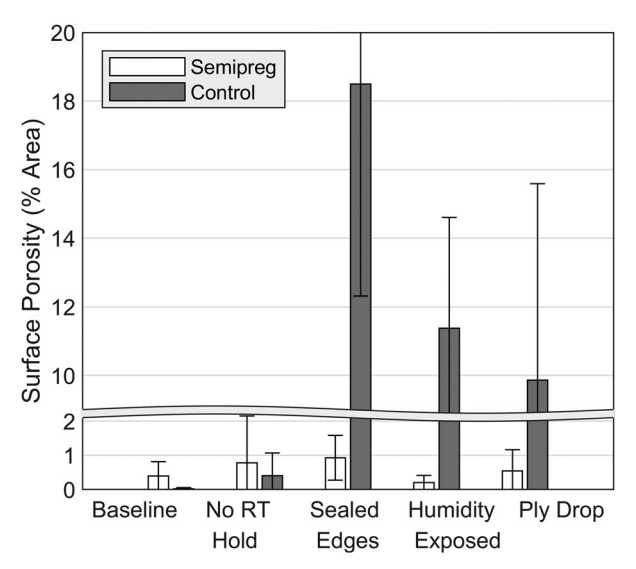


Figure 7. Surface defect content for semipreg and control prepreg laminates produced under baseline and a variety of sub-optimal conditions.

Differences in flow properties of semipreg and control resins emphasize the importance of prepreg format. Semipreg resin viscosity remained higher and gelled more rapidly than control resin, leaving less time (vs. control) for gas evacuation, resin flow, and fiber bed saturation. Resin rich regions remaining on the surface and interior of each sample indicate that resin flow did not reach equilibrium in semipreg laminates prior to gelation. The difference between flow properties make the processing window narrower for semipreg than the control resin, yet semipreg laminates were less sensitive to adverse processing conditions than control laminates. In principle, a semipreg produced with the control resin would be expected achieve more uniform resin distribution and fewer flow-related defects (see Type 2 void discussion below).

The results corroborate previous work indicating the importance of prepreg format in process robustness and expand on the prior work to provide evidence that the process robustness associated with through-thickness permeability is not limited to woven prepregs that have fiber tow crossings.

3.2.4. Thickness uniformity

The standard deviation of laminate thickness was found to be 12.9 µm and 19.3 µm for representative samples of control prepreg and semipreg, respectively. Normalized for average laminate thickness, this standard deviation in ply thickness corresponds to 0.59% and 0.74% of the average laminate thickness. These data indicate that semipregs can produce laminates of comparable thickness uniformity to commercially available prepregs. Furthermore, selection of a resin system more closely resembling the control resin is anticipated to reduce thickness variation in semipreg laminates below the minimal level observed in this study. By reaching a lower minimum viscosity and remaining at a low viscosity for longer prior to gelation, resin flow would be encouraged, resulting in more uniform resin distribution (and therefore, more uniform laminate thickness).

3.3. Void formation study

The primary void formation mechanisms for semipreg were visualized and identified, and their relationship with resin feature topography investigated by characterizing the surface quality of unmodified and modified formats of semipreg.

3.3.1. Defect formation

Figure 9 shows a series of images of the glass tool plate-prepreg interface. Images capture the formation

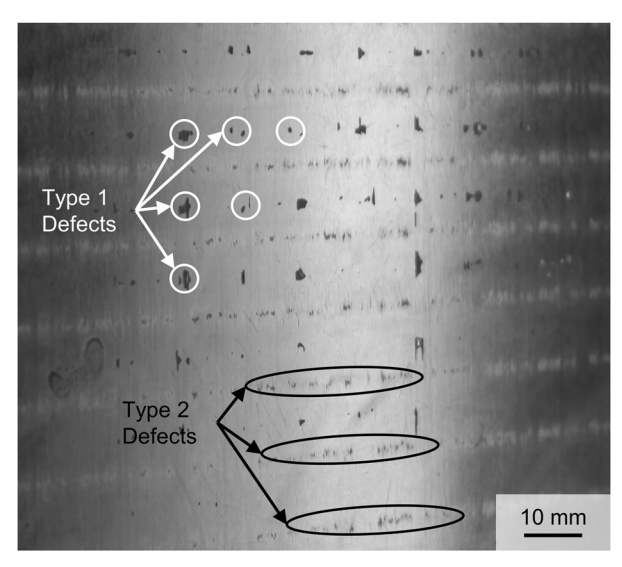


Figure 8. Image of the surface of the Ply Drop semipreg laminate indicating each of the two types of surface defects found in semipreg laminates.

and movement of both types of voids observed in semipreg laminates.

3.3.2. Type 1 voids

Type 1 voids were formed by entrapment of gas between resin strips and the tool plate and are circled in solid white in Figure 9. The first image in Figure 9 shows thin (in the z-direction) pockets of gas present at the interface of resin strips and the tool plate immediately after layup. During the fourhour RT-VH, the shape and location of these gas pockets evolved: voids tended to move toward the center of resin strips, decrease in area, and increase in depth. Upon heating, further distortion of voids occurred according to the same trend until gelation. Once formed during the initial layup and vacuum hold, entrapped gases at the tool-resin strip interface remained throughout cure and appeared in the laminate as Type 1 voids.

Type 1 defects were distributed quasi-periodically: along the length of each resin strip and transversely aligned across strips. Periodicity and alignment indicate that movement of entrapped gases during cure was determined by resin distribution (e.g. strip width, orientation, and spacing). Defect formation is attributed to local variations in compaction that arise from step-like variability in local ply thickness. Compaction forces are greatest along the strip edges (due to fiber bridging), and such forces are additive at the intersection of resin strips on adjacent plies. Intersections of orthogonal resin strips on adjacent plies create areas of greater compaction force that drive entrapped gases to the respective midline of each strip. This mechanism explains why Type 1 voids occurred primarily in locations corresponding to the intersection of strips on the tool side ply and its nearest neighbor.

The nature of gas entrapment and migration that produces Type 1 voids in semipreg laminates indicates that two mitigation strategies may be effective: (1) minimizing the volume of gas initially entrapped between resin features and (2) modifying resin features such that stress concentrations drive voids away from resin strip midlines.

3.3.3. Type 2 voids

Type 2 voids were located at interfaces of resin flow fronts between each adjacent resin strip. Figure 9 shows the degree of fiber bed saturation between adjacent resin strips at various times during processing, and the locations of two Type 2 voids are highlighted with dashed circles. In these images, Type 2 voids are observed to result from insufficient resin flow into areas of the fiber bed between strips.

Multiple factors can contribute to the formation of Type 2 defects. First, semipreg resin may not have had an appropriate rheological profile to enable reliable saturation of the region between resin strips. Type 2 defects were observed in regions of the laminate furthest away from the initial position of resin. Such regions require the most time for resin infiltration and may remain unsaturated if gelation occurs too rapidly. Surface defect measurements show that a prepreg with shorter resin flow distances produces laminates with lower Type 2 defect content: Type 2 defect content was roughly an order of magnitude less for the Humidity Exposed laminate than for any other semipreg sample. During conditioning of the Humidity Exposed semipreg, resin flow widened each resin strip, reducing the distance between strips by approximately 50% (Figure 10, discussed more thoroughly below) prior to layup. The correlation between resin flow distance and Type 2 defect content supports the hypothesis that Type 2 defects are caused by insufficient flow prior to gelation.

An alternative or additional explanation for the formation of Type 2 defects is that evacuation pathways may have been sealed prior to full removal of gas from the layup. Once evacuation paths are saturated with resin, any remaining gas in a sealed (but unsaturated) volume of the fiber bed would remain entrapped. When unsaturated regions shrink during impregnation, gas pressure increases until an equilibrium is reached, halting impregnation prior to full saturation and resulting in voids. Finally, the formation of Type 2 defects may have also been influenced by the local variations in compaction pressure in the layup created by step-like discontinuities in ply thickness. Ply thickness variations are anticipated to create regions of relatively lower compaction pressure in areas of prepreg plies between resin strips. The occurrence of Type 2 voids may be

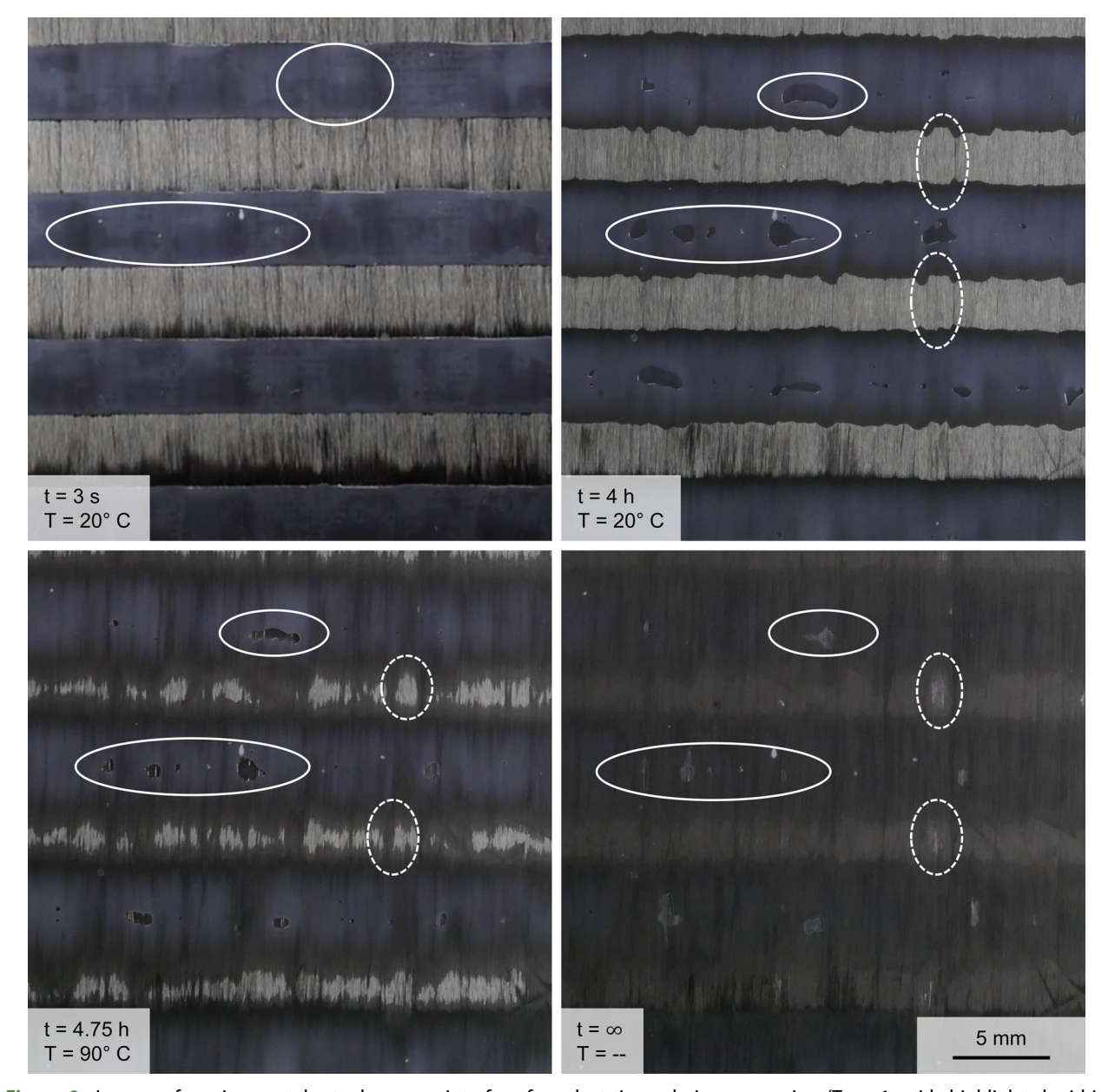


Figure 9. Images of semipreg at the tool-prepreg interface for select times during processing (Type 1 voids highlighted within solid circles, Type 2 voids highlighted within dashed circles).

explained by insufficient local compaction forces between resin strips at the ply-tool interface. More work is needed to confirm the operation and relative importance of these mechanisms.

The nature and evolution of the unsaturated regions resulting in Type 2 defects in semipreg laminates indicates that defect levels can be reduced by (1) selecting a resin system with lower viscosity and/ or delayed gelation or (2) reducing the distance between resin strips.

3.3.4. Resin topography and surface porosity

Figure 11 presents surface porosity data for semipreg, SPA, SPB, and SPC laminates. Modifying the cross-sectional shape of resin strips to resemble a bell curve vs. a rectangle (SPA) and modifying the resin surface topography to contain gas evacuation channels (SP_C) both reduced the number of defects

relative to the laminate produced from unmodified semipreg. Process monitoring verified that void reduction was caused by less air entrapment (vs. semipreg) at the tool-strip interface during layup of SP_A. Further, stress concentrations created by locally variable ply thickness were not as extreme in SPA (vs. semipreg) because of the rounding of strip edges, which reduced the tendency to immobilize gases in the center of strips. In the case of SP_C, entrapped gases were near evacuation channels created by the interconnected network of depressions embossed on resin strip surfaces. These depressions acted as gas removal channels, resulting in fewer, smaller surface defects in SPC laminates than observed for semipreg laminates. Pressing semipreg with smooth (SPA) and crosshatch (SPC) release paper resulted in laminates with equivalent surface quality of 0.08% and 0.12%, respectively.

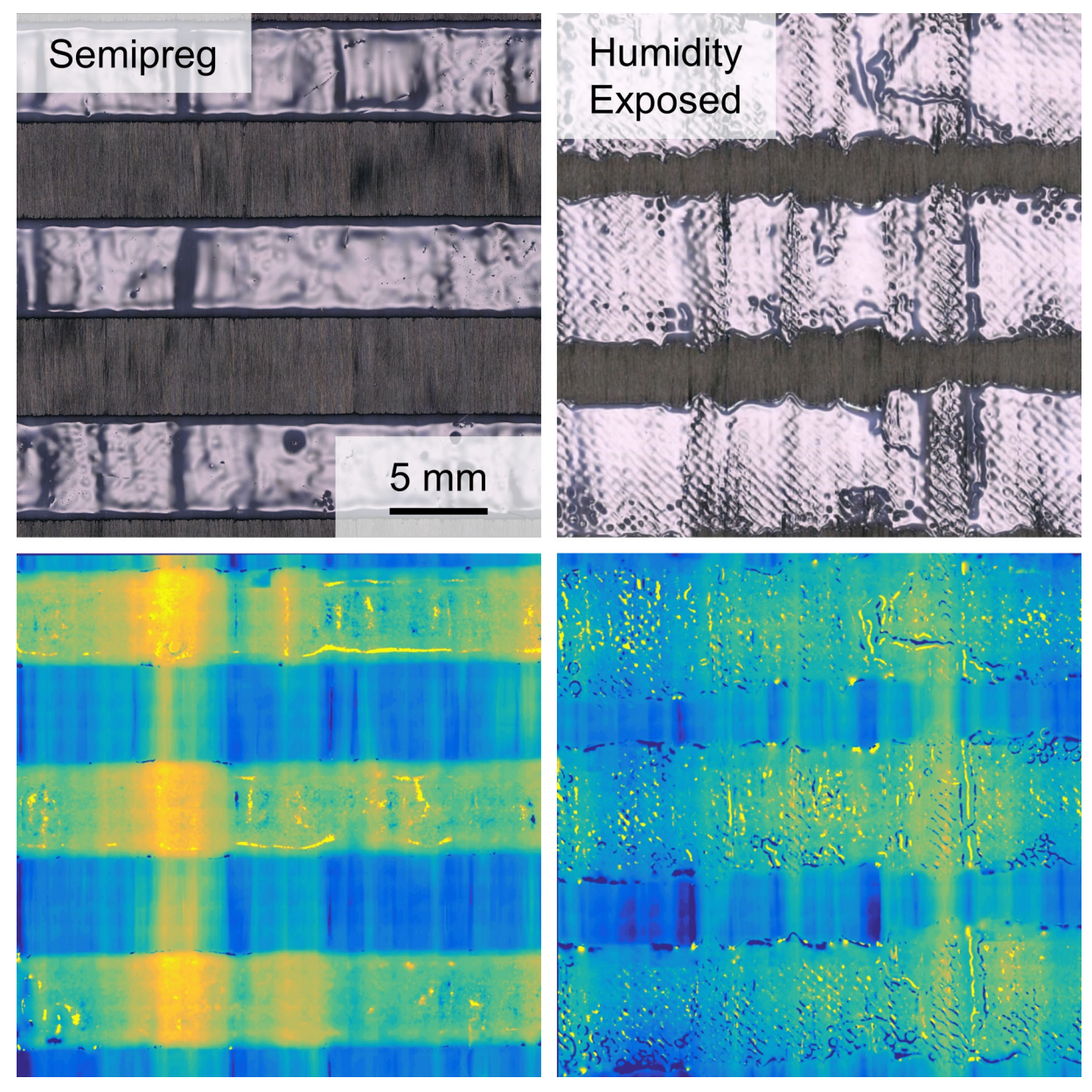


Figure 10. Comparison of resin strips on semipreg before and after conditioning at 35 °C and 90% relative humidity for 24 h.

Semipreg modified by pressing with diamondtextured release paper (SPB) produced the laminate with the highest void content (1.54%). The roughly threefold increase in surface porosity compared to semipreg was attributed to the resin strip topography: diamond shaped impressions left by release paper in resin strips on SP_B (1) increased the volume of air entrapped during layup and (2) immobilized entrapped gases by sealing the resin strip-tool interface, creating distinct, unconnected voids. Entrapped gases were never effectively removed during processing and resulted in Type 1 voids in the cured laminate.

3.3.5. Discussion

Observations of resin flow during processing provided insight into the mechanisms involved in formation of surface defects. Type 1 voids were produced from gases entrapped at the resin strip-

tool plate interface during layup and never removed. Type 2 voids were related to the flow properties and spacing of resin features on semipreg. Resin strip topography played a critical role in the formation of Type 1 voids, and changes in resin strip cross section and the embossment of interconnected evacuation channels onto resin strip surfaces were both effective methods to reduce surface porosity.

The mechanisms by which surface defects form, as identified here, may also cause bulk defects. The correlation between bulk defect location and resin strip distribution, as revealed by microtomography, supports this hypothesis. Both internal and surface defects had periodicity associated with the spacing of resin strips. Bulk defects can be produced via a mechanism analogous to that which produce Type 1 surface defects: instead of gas entrapment occurring at the tool-resin strip interface, it occurs at the interface of resin strips on adjacent plies.

The assertion that similar mechanisms produce surface and bulk defects is supported by bulk porosity data from Humidity Exposed semipreg. The reduction in surface defect content between Humidity Exposed and Baseline semipreg was initially attributed to an assumed reduction in resin tack, which has been previously correlated with surface porosity [24]. Such phenomena, however, do not fully explain the observed reduction in bulk porosity (relative to Baseline semipreg), where moisture absorbed during humidity conditioning was anticipated to volatilize during cure, increasing void content over Baseline semipreg.

Rather than tack reduction, changes in resin strip topography were responsible for minimal defect content in Humidity Exposed semipreg. Figure 10 shows micrographs and height maps highlighting changes in semipreg format resulting from exposure to elevated temperature and humidity. Softened strip edges and 50% increased strip width indicates resin flow occurred during conditioning. Furthermore, smooth strip surfaces were replaced with rough, uneven surfaces. Such features were identified in the Void Formation Study as associated with a reduction in defect content. Strip morphology changes during conditioning provide a compelling explanation for the unexpected quality of Humidity Exposed semipreg laminates. These results indicate that resin feature topography can be a more significant factor in determining void content than the presence of excess moisture (due to improper handling or storage).

4. Conclusions

This work demonstrated a method for producing semipreg with periodic distributions of resin. UD prepreg with resin strips orthogonal to the fiber direction enhanced through-thickness gas transport. Compared to a commercial hot-melt OoA prepreg, defect content in laminates cured from in-house produced prepreg was less sensitive to deviations from baseline cure conditions. The results indicate the efficacy of through-thickness permeability (and short egress pathways) for removal of entrapped or evolved gases from UD prepreg during cure. The evidence indicates that benefits imparted by high through-thickness permeability previously observed in woven fabrics do not require tow overlaps or underlaps, and such formats are similarly effective in UD fiber beds.

Process robustness was particularly notable, because no effort was made to optimize resin rheology or resin feature geometry (e.g. strips vs. grid), including spacing (i.e. periodicity of strips or grid)

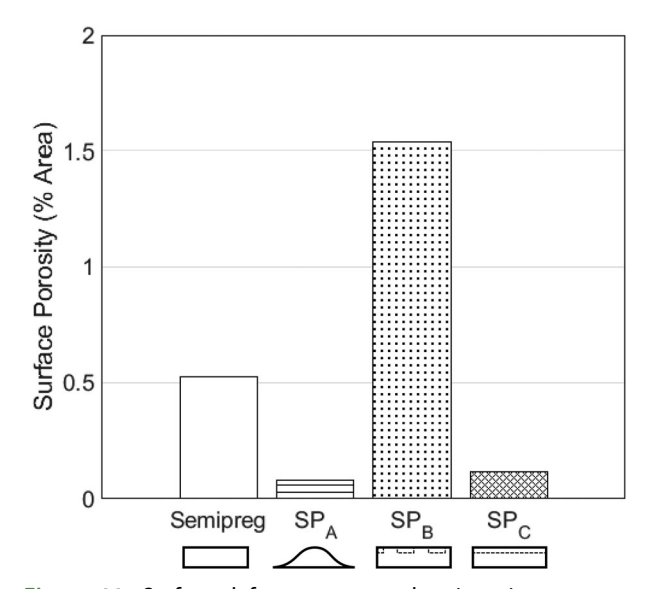


Figure 11. Surface defect content and resin strip cross section schematic for unmodified and modified semipreg laminates produced under baseline conditions.

and topography (i.e. resin feature cross section and surface texture). Such opportunities, however, were identified in the Void Formation Study.

In-situ process monitoring revealed the nature and origin of surface porosity in semipregs, and two distinct types of surface voids were identified. The mechanisms by which each void type formed was explained, attributing voids to either gas entrapment by resin features or insufficient resin flow during processing. Morphology of resin features played an important role in these mechanisms. Changes to resin strip cross section and the addition of evacuation pathways on resin feature surfaces each reduced defect content compared to unmodified semipreg. Microtomography data supported the hypothesis that similar defect formation mechanisms create both surface and bulk porosity, but further work is required to prove this.

This study suggests that next-generation prepreg formats may share several characteristics. Namely, next-generation prepregs formats must be designed to (1) limit gas entrapment during layup and (2) provide efficient through-thickness evacuation pathways. The first of these qualities can be achieved through careful control of resin feature morphology (e.g. ensuring resin features have a domed cross section to minimize bubble entrapment during layup). The second quality can be achieved by interrupting the continuity of resin distribution and by texturing resin features to have evacuation channels on their surface (as in SP_C). Resin features should have sufficient spacing to enable rapid through-thickness air evacuation but should also be close enough together to enable full fiber bed saturation between features during processing (minimizing Type 2 voids). Optimal spacing of resin features is anticipated to depend on



resin chemistry, processing parameters, and fiber bed architecture. More work is necessary to determine the relationship between these parameters.

Broadly, this work represents a step toward addressing the need for rapid, flexible, robust, and cost-effective high-performance composite manufacturing techniques. Growing demand for composite structures, limited availability of autoclaves, and the inherently unsuitable nature of autoclave processing in some scenarios (e.g. in-field repair, large structures) continue to drive the need for manufacturing methods with improved technical, cost, and environmental efficiency. The approach presented here effectively transfers the robustness of autoclave cure into the material itself, and further development will accelerate the adoption of VBO prepregs.

Disclosure statement

No potential conflict of interest was reported by the authors.

ORCID

William T. Edwards (D) http://orcid.org/0000-0002-9276-7406 Steven R. Nutt (D) http://orcid.org/0000-0001-9877-1978

References

- Molyneux M, Murray P, Murray B. Prepreg, tape and fabric technology for advanced composites. Composites. 1983;14(2):87-91.
- Steele M, Corden T, Gibbs A. The development of out-of-autoclave composite prepreg technology for aerospace applications. Proceedings of the SAMPE Technical Conference; 2011; Long Beach.
- Jackson K, Crabtree M. Autoclave quality composites tooling for composite from vacuum bag only processing. Proceedings of the 47th International SAMPE Symposium; 2002; Long Beach.
- Thorfinnson B, Biermann T. Degree of impregnation of prepregs - effects on porosity. Proceedings of the 32nd International SAMPE Symposium; 1987; Philadelphia.
- Repecka L, Boyd J. Vacuum-bag-only-curable prepregs that produce void-free parts. Proceedings of the SAMPE Technical Conference; 2002; Long Beach.
- Centea T, Grunenfelder LK, Nutt SR. A review of out-of-autoclave prepregs - material properties, process phenomena, and manufacturing considerations. Compos Part A Appl Sci Manuf. 2015;70:132-154.
- [7] Ridgard C. Out of autoclave composite technology for aerospace, defense and space structures. Proceedings of the SAMPE Technical Conference; 2009; Baltimore.
- Centea T, Hubert P. Out-of-autoclave prepreg consolidation under deficient pressure conditions. J Compos Mater. 2014;48(16):2033-2045.

- Grunenfelder LK, Nutt SR. Void formation in [9] composite prepregs - effect of dissolved moisture. Compos Sci Technol. 2010;70(16):2304-2309.
- [10] Cender TA, Simacek P, Davis S, et al. Gas evacuation from partially saturated woven fiber laminates. Transp Porous Med. 2016;115(3):541-562.
- Kay J, Fernlund G. Process Conditions and Voids in [11] out of Autoclave Prepregs. Proceedings of the SAMPE Technical Conference; 2012; Baltimore. p. 12.
- [12] Grunenfelder LK, Fisher C, Cabble C, et al. Defect control in out-of-autoclave manufacturing of structural elements. Proceedings of the SAMPE 2012 Technical Conference; 2012; Charleston.
- Ma Y, Centea T, Nilakantan G, et al. Vacuum Bag [13] Only Processing of Complex Shapes: Effect of Corner Angle, Material Properties and Process Conditions. Proceedings of the 29th Technical Conference of the American Society for Composites/16th US-Japan Conference on Composite Materials/ASTM D-30 Meeting; 2014; San Diego. p. 2-17.
- [14]Tavares SS, Michaud V, Månson J-AE. Assessment of semi-impregnated fabrics in honeycomb sandwich structures. Compos Part A Appl Sci Manuf. 2010;41(1):8-15.
- [15] Grunenfelder LK, Dills A, Centea T, et al. Effect of prepreg format on defect control in out-of-autoclave processing. Compos Part A Appl Sci Manuf. 2017;93:88-99.
- [16] Howard S. Evaluating consolidation dynamics study of key consolidation parameters in a vacuum bag only (VBO) cure. Proceedings of the SAMPE 2016 Technical Conference; 2016; Long Beach.
- Anders M, Zebrine D, Centea T, et al. In-situ [17] observations and pressure measurements for autoclave co-cure of honeycomb core sandwich structures. Proceedings of the ASME 2017 Manufacturing International Science and Engineering Conference; 2017; Los Angeles.
- [18] Tavares SS, Caillet-Bois N, Michaud V, et al. Nonautoclave processing of honeycomb sandwich structures: skin through thickness air permeability during cure. Compos Part A Appl Sci Manuf. 2010;41(5):646-652.
- [19] Tavares SS, Michaud V, Månson JAE. Through thickness air permeability of prepregs during cure. Compos Part A Appl Sci Manuf. 2009;40(10):1587-1596.
- [20] Kim D, Centea T, Nutt SR. Out-time effects on cure kinetics and viscosity for an out-of-autoclave (OOA) prepreg: modelling and monitoring. Compos Sci Technol. 2014;100:63-69.
- [21] Kratz J, Hubert P. Anisotropic air permeability in out-of-autoclave prepregs: effect on honeycomb panel evacuation prior to cure. Compos Part A Appl Sci Manuf. 2013;49:179-191.
- [22] Louis B, Hsiao K, Fernlund G. Gas permeability measurements of out of autoclave prepreg MTM45-1/CF2426A. Proceedings of the SAMPE Technical Conference; 2010; Seattle.
- [23] Irving, P. E., and Soutis, C., eds. Polymer composites in the aerospace industry. Sawston, Cambridge: Woodhead Publishing; 2019.
- Hamill L, Centea T, Nutt S. Surface porosity dur-[24] ing vacuum bag-only prepreg processing: causes and mitigation strategies. Compos Part A Appl Sci Manuf. 2015;75:1-10.